Coincidence of magnetic and valence quantum critical points in $CeRhIn_5$ under pressure

Z. Ren,[1,2,*] G. W. Scheerer,[1] D. Aoki,[3,4] K. Miyake,[5] S. Watanabe,[6] and D. Jaccard[1]

[1] *DQMP–University of Geneva, 24 Quai Ernest-Ansermet, CH-1211 Geneva 4, Switzerland*

[2] *Institute for Natural Sciences, Westlake Institute for Advanced Study, 18 Shilongshan Road, Hangzhou, People's Republic of China*

[3] *Université Grenoble Alpes, Commissariat à l' Energie Atomique et aux Energies Alternatives (CEA), Institut Nanosciences et Cryogenie (INAC)-PHELIOS, F-38000 Grenoble, France*

[4] *Institute for Materials Research, Tohuko University, Oarai, Ibaraki 311-1313, Japan*

[5] *Center for Advanced High Magnetic Field Science, Osaka University, Toyonaka 560-0043, Japan*

[6] *Department of Basic Sciences, Kyushu Institute of Technology, Kitakyushu 804-8550, Japan*

(Received 15 September 2017; revised manuscript received 20 November 2017; published 28 November 2017)

We present accurate electrical resistivity measurements along the two principle crystallographic axes of the pressure-induced heavy-fermion superconductor $CeRhIn_5$ up to 5.63 GPa. For both directions, a valence crossover line is identified in the p-T plane and the extrapolation of this line to zero temperature coincides with the collapse of the magnetic ordering temperature. Furthermore, it is found that the p-T phase diagram of $CeRhIn_5$ in the valence crossover region is very similar to that of $CeCu_2Si_2$. These results point to the essential role of Ce-4f electron delocalization in both destroying magnetic order and realizing superconductivity in $CeRhIn_5$ under pressure.

DOI: 10.1103/PhysRevB.96.184524

I. INTRODUCTION

The occurrence of pressure-induced superconductivity (SC) in Ce-based heavy-fermion (HF) compounds has attracted a lot of attention in the field of condensed matter physics [1]. For most of such materials, SC appears in the vicinity of a magnetic quantum critical point (QCP) at p_c, leading to the belief that spin fluctuations are responsible for the Cooper pairing [2]. On the other hand, Ce-valence fluctuations may also act as the pairing glue [3] and the corresponding critical endpoint (CEP) at p_v can be deduced by resistivity scaling analysis [4]. It is noteworthy that the relative position between p_c and p_v may vary for different systems, probably depending on the hybridization strength (V) between Ce-4f and conduction electrons [5,6]. For example, while p_c and p_v are well separated in $CeCu_2Si_2$ [3] and $CeCu_2(Si_{1-x}Ge_x)_2$ [7], they are very close in $CeAu_2Si_2$ [8].

$CeRhIn_5$ belongs to the Ce-115 family, whose structure consists of alternating $CeIn_3$ and $RhIn_2$ layers stacked along the c axis [9]. At ambient pressure, the compound is a prototypical heavy-fermion antiferromagnet with a Néel temperature $T_N = 3.8$ K, although a signature of SC was reported at $\sim$90 mK [10]. Under pressure, the T_N of $CeRhIn_5$ passes through a maximum and disappears at $\sim$2 GPa, above which the antiferromagnetic order is rapidly suppressed as confirmed by the NQR measurement [11]. Meanwhile, SC is observed over a broad pressure range with a maximum T_c of 2.3 K at $p_c \approx 2.5$ GPa [9]. Although experimental signatures for the existence of a QCP are found at p_c, the nature of fluctuations remains under debate [12,13]. In particular, de Haas-van Alphen (dHvA) measurements detect an abrupt change in the Fermi surface shape across p_c [14], yet the resistivity above T_c remains nearly isotropic [13]. This is hardly understood within the common picture of magnetic quantum criticality. Instead, Park *et al.* attribute this p_c to a Kondo breakdown QCP, at which the whole heavy Fermi surface is destroyed [13]. Alternatively, Watanabe and Miyake proposed theoretically that the coincidence of p_c and p_v is responsible for these anomalous behaviors [15].

In order to shed light on this issue, we carried out simultaneous measurements of the a- and c-axis electrical resistivity of $CeRhIn_5$ in a single pressure cell up to 5.63 GPa. For both directions, analysis of the resistivity data allows us to draw the valence crossover line in the p-T phase diagram. Moreover, a scaling behavior is observed for the a-axis data, providing clear evidence for the existence of a CEP located at $p_v = 2.6 \pm 0.1$ GPa and slightly negative temperature. Our results support the scenario that p_v and p_c are nearly identical in $CeRhIn_5$. In addition, a comparison with $CeCu_2Si_2$ is made, and its implication on the pairing mechanism is discussed.

II. EXPERIMENTAL

High quality $CeRhIn_5$ and $LaRhIn_5$ crystals were grown by the In-flux method [12]. After carefully removing the residual flux, crystals were oriented and cut along the a and c axis, respectively. The high-pressure experiment was performed using a Bridgman-type tungsten carbide anvil cell with Daphne oil as hydrostatic pressure medium and Pb as pressure gauge [16]. Both samples and a Pb gauge were connected in series, and their resistivities were measured at temperatures from 300 down to 1.2 K by the standard four-probe method. Throughout the experiments, the pressure gradient estimated from the width of the Pb superconducting transition was less than 0.05 GPa. To determine better the absolute resistivity value, pressure-dependent resistivity at 292 K was extrapolated to $p = 0$. The obtained value was corrected by the one measured at ambient condition, yielding a normalization factor for the results under pressure. Thanks to this special care, the estimated error in the absolute resistivity value is within 2%.

*zhi.ren@wias.org.cn

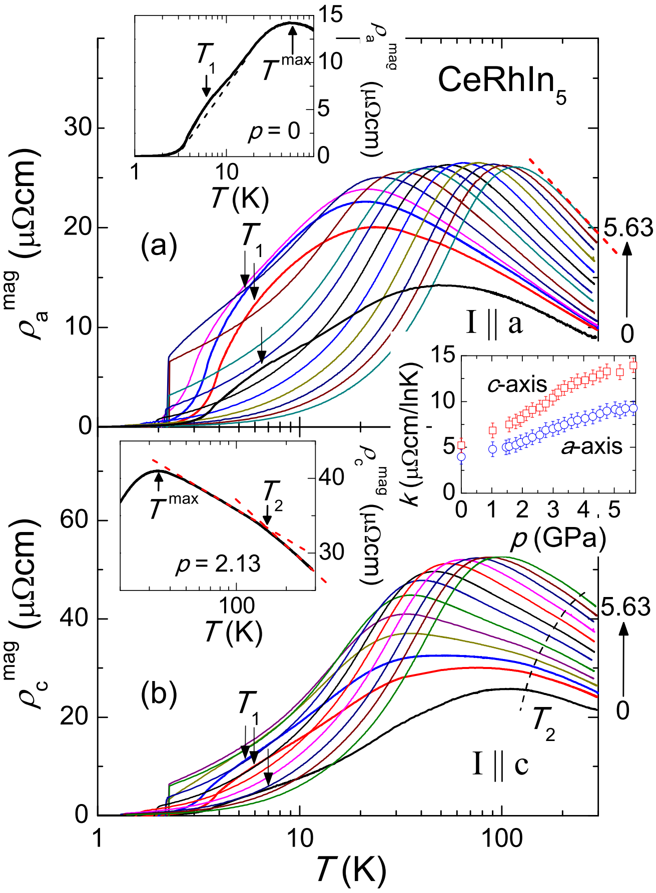

FIG. 1. Logarithmic T dependence of the magnetic resistivity of $CeRhIn_5$ along the (a) a and (b) c axis under pressures up to 5.63 GPa. The arrows and the dashed line are a guide to the eyes. The inset of (a) shows the a-axis data at $p = 0$. The resistivity maximum and bump are marked by $T^{\max}$ and T_1, respectively. The dashed line is a guide to the eyes. The inset of (b) shows the c-axis data at $p = 2.13$ GPa. The two dashed lines indicate the $-\ln T$ slope, and their intersection temperature is marked as T_2. The inset in between (a) and (b) shows the pressure dependencies of the $-\ln T$ slope below room temperature for both axes.

III. RESULTS AND DISCUSSION

Figure 1 shows the temperature dependencies of the magnetic resistivity $\rho^{\text{mag}} = \rho(\text{CeRhIn}_5) - \rho(\text{LaRhIn}_5)$ of $CeRhIn_5$ at pressures up to 5.63 GPa. The weak pressure variation of $\rho(\text{LaRhIn}_5)$ is taken into account following Ref. [13]. In general, the pressure evolution of ρ^{mag} is reminiscent of that observed in other Ce-based Kondo lattice compounds. At $p = 0$, ρ_a^{mag} exhibits a $-\ln T$ dependence below room temperature, reflecting incoherent Kondo scattering on excited crystal field (CF) levels [17]. Upon further cooling, a broad maximum is observed at $T_{\max}$ and a small bump is discernible at a lower temperature T_1, which is defined empirically as 3/4 of the temperature at which the second derivative of ρ^{mag} reaches a maximum. With increasing pressure, T_1 decreases modestly and becomes no longer resolvable above 1.57 GPa, while $T_{\max}$ first decreases then increases. In addition, a signature of magnetic ordering is observed below 1.78 GPa, while a superconducting transition occurs between 1.03 and 3.80 GPa.

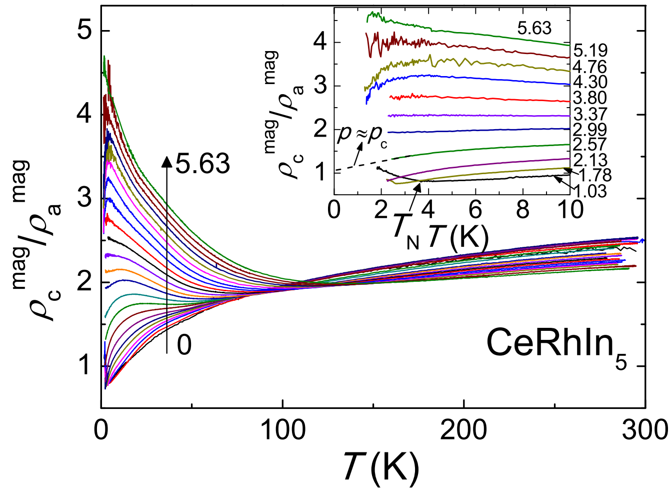

FIG. 2. Temperature dependencies of the magnetic resistivity anisotropy under pressures up to 5.63 GPa. The inset shows a zoom of the data below 10 K at selected pressures. The dashed line is an extrapolation of the curve at $p \approx p_c$ to zero temperature.

As can be seen in Fig. 1(b), ρ_c^{mag} behaves similarly to ρ_a^{mag}, except that the former displays two different $-\ln T$ dependencies above $T_{\max}$. This new observation is likely due to the relatively small value of the first CF splitting energy in comparison with other Ce-based HF systems [18]. Extrapolations of these $-\ln T$ behaviors intersect at the temperature T_2 [inset of Fig. 1(b)], which increases with pressure. Nevertheless, for both axes, the $-\ln T$ slope k near room temperature grows by nearly the same factor of 3 up to 5.63 GPa, which signifies a strong enhancement of the Kondo coupling by pressure [17].

Figure 2 shows the anisotropy of the magnetic resistivity $\gamma_{\text{mag}} = \rho_c^{\text{mag}}/\rho_a^{\text{mag}}$ plotted as a function of temperature under pressures up to 5.63 GPa. At $p = 0$, γ_{mag} decreases from $\sim$2.2 to < 1 with decreasing temperature and shows an upturn below T_N. This upturn, whose origin remains unclear at present, was not observed in the previous study [19]. Under pressure, the evolution of γ_{mag} is very similar to that of [13], and exhibits qualitative difference at temperatures above and below $\sim$120 K. For $T > 120$ K, γ_{mag} is weakly temperature and pressure dependent, and hence is likely dominated by the crystalline anisotropy.

By contrast, below $\sim$120 K, γ_{mag} increases strongly with increasing pressure and decreasing temperature. Consequently, the temperature dependence of γ_{mag} changes its curvature from downward to upward. At 2 K, the γ_{mag} value grows by a factor of 3 throughout the investigated pressure range (inset of Fig. 2). This feature can likely be understood by taking into account the anisotropic hybridization between Ce-4f electrons and conduction electrons [20]. Following such an interpretation, the hybridization strength grows much faster with pressure along the c axis than along the a axis. Nevertheless, at $p = 2.57$ GPa, the γ_{mag} value extrapolated to 0 K is very close to 1, pointing to isotropic magnetic scattering around p_c [13].

We now turn the attention to the low-temperature resistivity. Specifically, the ρ_a and ρ_c data are fitted by the power law $\rho = \rho_0 + AT^n$ [21], where ρ_0 is the residual resistivity, A the coefficient, and n the temperature exponent. As shown

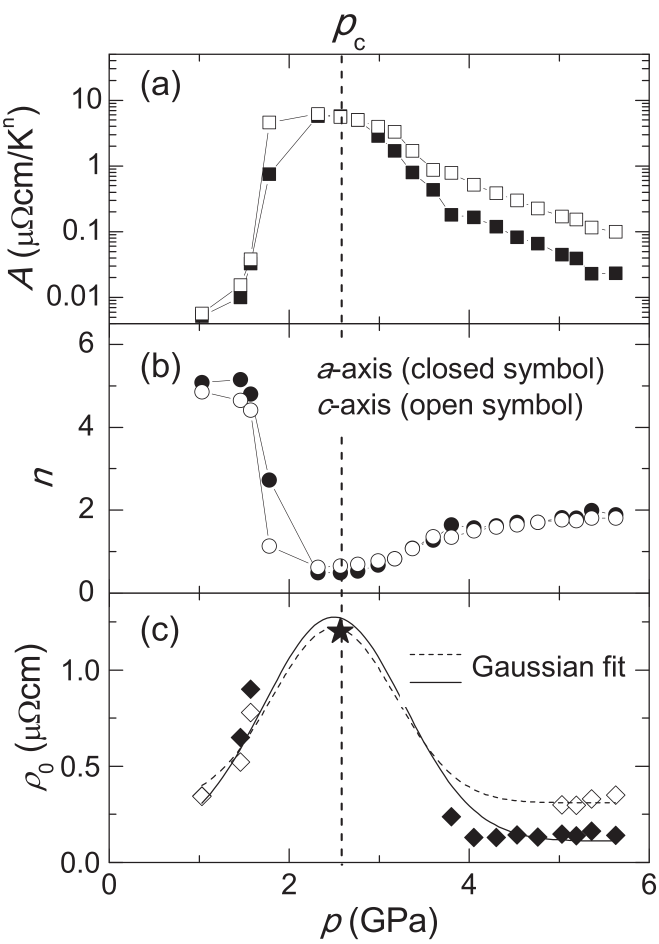

FIG. 3. (a)–(c) The pressure dependencies of the coefficient A, temperature exponent n, and residual resistivity ρ_0, respectively, obtained by fitting with the power law $\rho(T) = \rho_0 + AT^n$ to the a- (closed symbol) and c-axis (open symbol) resistivity data at low temperature. Note that the high-field value at 2.57 GPa in (c) is taken from Ref. [12] and assumed to be isotropic.

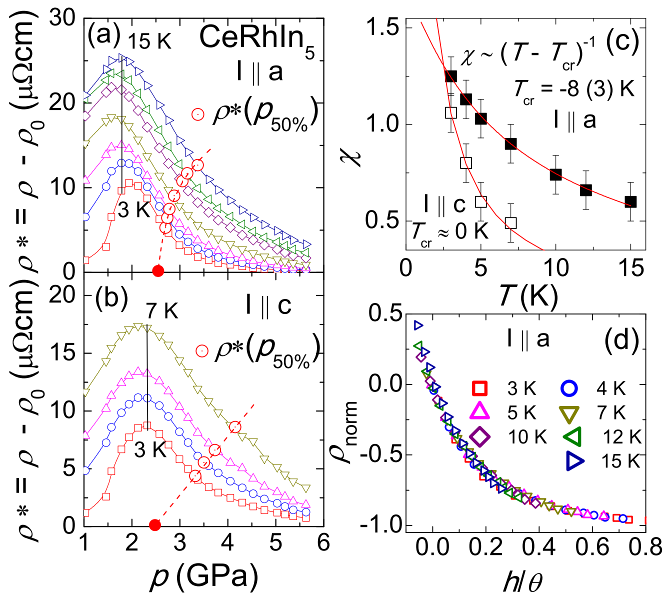

FIG. 4. (a) and (b) The isothermal $\rho^*(p) = \rho(p) - \rho_0(p)$ for the a and c axis at selected temperatures, respectively. The vertical solid lines mark the initial pressure of the valence crossover. The solid circles denote the 50% drop compared to the maximum ρ^* value, and the dashed lines are extrapolations of the circles to p_v. (c) Temperature dependencies of the slope χ for both axes (see text). The Curie-Weiss fitting yields $T_{cr} \approx -8$ K and 0 K for the a and c axis, respectively. (d) Collapse of a-axis normalized data ρ_{norm} when plotted against h/θ, where $h = (p - p_{50\%})/p_{50\%}$ and $\theta = (T - T_{cr})/|T_{cr}|$.

in Fig. 3, the resulting parameters display a similar pressure dependence along different axes. At $p \leqslant 1.57$ GPa, n is as large as $\sim$5, indicating dominant electron-magnon scattering due to the magnetic ordering. With increasing pressure above 1.57 GPa, since the magnetic ordering is rapidly suppressed, n decreases steeply and A increases accordingly. Around p_c, n shows a minimum of $\sim$0.6 while A is enhanced by $\sim$3 orders of magnitude. This non-Fermi liquid behavior is in good agreement with the previous results [13], pointing to the presence of quantum critical fluctuations. Although ρ_0 obtained from the fitting is negative and hence unphysical between 2.57 and 3.80 GPa, a value near p_c can be estimated from Ref. [12], in which SC can be completely suppressed by applying high magnetic fields. When plotted in Fig. 3(c), this evidences an enhanced scattering around p_c, as expected [22]. At pressures above $\sim$4 GPa, n becomes not far from the Fermi liquid value $n = 2$. In this pressure range, the drop in A by more than one order of magnitude up to 5.63 GPa is reminiscent of the case of $CeCu_2Si_2$ above p_v, and reflects a drastic enhancement of the $4f$ electron interactions [3].

To gain more insight, we plot the low-temperature isothermal resistivity $\rho^*(p) = \rho(p) - \rho_0(p)$ at selected temperatures in Figs. 4(a) and 4(b). A maximum is observed around 1.78 and 2.32 GPa for the a and c axes, respectively. At higher pressures, ρ^* decreases steeply without saturation, even in the paramagnetic state. This is again similar to that observed in $CeCu_2Si_2$ above 4 GPa, and, together with the rapid collapse of the A coefficient shown above, provides strong evidence for the proximity to a valence CEP located at (p_{cr}, T_{cr}) in the p-T plane of $CeRhIn_5$ [4].

The existence of such a CEP can be further corroborated by a scaling analysis outlined in Ref. [4]. Following the procedure, we define $p_{50\%}$ as the pressure corresponding to 50% of the resistivity drop compared to the value at 1.78(2.32) GPa for the a(c)-axis data, and ρ_{norm} as $\rho_{norm} = [\rho^* - \rho^*(p_{50\%})]/\rho^*(p_{50\%})$. As can be seen in Fig. 4(c), the slope $\chi = |\, d\rho_{norm}/dp \,|$ at $p_{50\%}$ increases with decreasing temperature, indicating that the ρ_{norm} decrease is getting steeper on cooling. Assuming $\chi \propto (T - T_{cr})^{-1}$, we obtain $T_{cr} \approx -8$ K and 0 K for the a and c axes, respectively. The scaling analysis consists of plotting ρ_{norm} against h/θ, where $h = (p - p_{50\%})/p_{50\%}$ and $\theta = (T - T_{cr})/|T_{cr}|$ are the generalized distance from the CEP. It turns out that all the a-axis ρ_{norm} isothermals below 15 K collapse on a single scaling curve [23]. This provides strong evidence for the existence of a CEP in the p-T plane of $CeRhIn_5$. The fact that T_{cr} is slightly negative for the a axis means that a crossover (COV) rather than a first-order transition occurs. In this respect, the temperature dependence of $p_{50\%}$ defines the

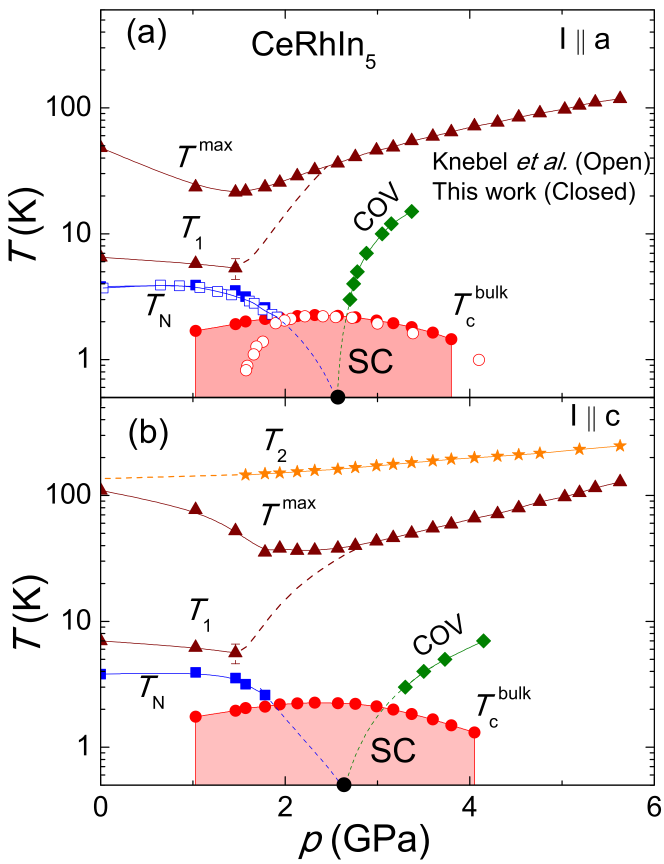

FIG. 5. Pressure-temperature phase diagram of CeRhIn$_5$ along the (a) a and (b) c axes, including the characteristic temperatures T_1, T_2, and T^{max}. For comparison, data from Ref. [12] are also included in (a).

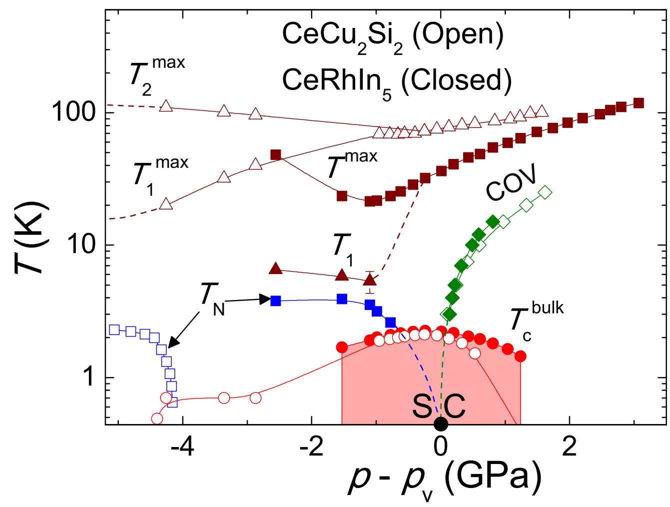

FIG. 6. Comparison of the in-plane pressure-temperature phase diagrams of CeRhIn$_5$ and CeCu$_2$Si$_2$ [4]. Note that p_v is set as the zero on the horizontal axis for both cases.

valence COV line (see below), and its extrapolation to zero temperature yields $p_v(\approx p_{cr}) = 2.6 \pm 0.2$ GPa for both cases. Notice that this p_v is determined from the results at much higher temperature than T_N, yet it is nearly identical to p_c.

The above results are summarized in the p-T phase diagrams (PD) shown in Fig. 5. Overall, the PDs look very similar along the two crystallographic directions. The normal-state behavior, characterized by the T_N, T_1, T^{max} and valence COV lines, is qualitatively similar to other Ce-based Kondo lattices [8]. At low pressure, as always observed, both T^{max} and T_1 decreases. For T_1, this is due to the increasing influence of the spin disorder scattering. On the other hand, the depression of T^{max} is ascribed to the rapid growing of the resistivity magnitude at T_1 as the Kondo temperature T_K rises. In this pressure range, T^{max} is primarily governed by the CF splitting Δ_{CF}. But at pressures above p_v, since the resistivity contribution at T_1 starts to dominate, the T_{max} line merges with that of T_1 and becomes an indication of T_K [3].

Strikingly, for both directions, the T_N and COV lines terminate at almost the same point on the horizontal axis. In other words, the magnetic QCP at p_c nearly coincides with the valence CEP at p_v, as already noted. Here we emphasize that the pressure evolution of T_N is in excellent agreement with a previous study [12], although a wider superconducting window is observed in our case. Actually, we have also performed measurements of the a-axis resistivity under pressure on a crystal from Thompson's group [9], and found identical results as those presented in this paper and notably $p_c \approx p_v$. Hence this coincidence appears to be an intrinsic property of CeRhIn$_5$, and substantiates that the pressure-induced delocalization of the Ce 4f electron is the driving force for the collapse of the magnetic ordering in this material.

Theoretically, it has been shown that, for Ce-based periodic Anderson lattices with a large V, p_c, and p_v are separated in the p-T PD [5]. As V decreases, p_c approaches p_v and finally the two pressures coincide, which is thought to correspond to the case of CeRhIn$_5$. It is noted that in CeIrIn$_5$, which appears to have a larger V than CeRhIn$_5$, the In nuclear quadruple resonance (NQR) measurement suggests the existence of the valence COV line near 2 GPa [24], while its p_c is believed to be located at negative pressure [25]. Hence our results are in a broad agreement with previous theoretical and experimental studies. Furthermore, according to Watanabe and Miyake [5], the coincidence of p_c and p_v consistently explains the anomalous properties observed in CeRhIn$_5$ by the dHvA measurement, including the Fermi surface change and the cyclotron mass enhancement [14].

Another salient feature of Fig. 5 is that although T_N and T_c are isotropic, the COV line is sharper along the a axis than along the c axis. Naively, this is expected since the Ce-Ce distance is the shortest along the a axis. Hence the nucleation of valence COV develops more rapidly in this direction. A better understanding of this issue may require further studies of the valence COV line by other probes such as NQR [24,26], as well as elaborated theoretical treatments in the future.

Finally, we present in Fig. 6 a comparison between in-plane p-T diagrams of CeRhIn$_5$ and CeCu$_2$Si$_2$. Compared with the T_1^{max} and T_2^{max} lines of CeCu$_2$Si$_2$, the T^{max} and T_1 lines of CeRhIn$_5$ are systematically lower, which is likely due to the smaller value of the first CF splitting energy [18]. Nevertheless, in both cases, the two lines merge in the vicinity of p_v. At higher pressures, the T_c and COV lines as a function of the distance from p_v are nearly identical for these two compounds. This is quite remarkable considering their different crystal structures, and hence points to a common superconducting pairing mechanism. Note that, just below p_v, magnetic ordering is present in $CeRhIn_5$, but is absent in $CeCu_2Si_2$. It is thus tempting to speculate that, around the optimal pressure for superconductivity of $CeRhIn_5$, valence fluctuations play a more important role than spin fluctuations in the Cooper pairing, although both of them are expected to be present.

IV. CONCLUSION

In summary, we have studied the a- and c-axis resistivity of $CeRhIn_5$ under pressure up to 5.63 GPa. A careful data analysis enables us to add the valence crossover line and to locate the CEP at 2.6 GPa and slightly negative (zero) temperature in the p-T plane. For the a axis, a resistivity scaling is observed, and the updated phase diagram in the COV regime is very similar to that of $CeCu_2Si_2$. Our results provide first experimental evidence that the magnetic QCP and valence CEP coincide with each other in $CeRhIn_5$, which highlights the importance of Ce-4f electron delocalization in understanding the pressure evolution of magnetism and superconductivity in this material.

ACKNOWLEDGMENTS

We acknowledge J. Flouquet for enlightening discussions, and M. Lopez and S. Müller for technical support. S.W. is supported by the Grant-in-Aid for Scientific Research (Grants No. 24540378, No. 15K05177, and No. 16H10177) from the Japan Society for the Promotion of Science (JSPS), and by JASRI (Grant No. 0046 in 2012B, 2013A, 2013B, 2014A, 2014B, and 2015A). K.M. is supported by a grant from JSPS (Grant No. 17K05555).

[1] G. Knebel, D. Aoki, and J. Flouquet, C. R. Phys. **12**, 542 (2011).
[2] N. D. Mathur, F. M. Grosche, S. R. Julian, I. R. Walker, D. M. Freye, R. K. W. Haselwimmer, and G. G. Lonzarich, Nature (London) **394**, 39 (1998).
[3] A. T. Holmes, D. Jaccard, and K. Miyake, Phys. Rev. B **69**, 024508 (2004).
[4] G. Seyfarth, A.-S. Ruetschi, K. Sengupta, A. Georges, D. Jaccard, S. Watanabe, and K. Miyake, Phys. Rev. B **85**, 205105 (2012).
[5] S. Watanabe and K. Miyake, J. Phys.: Condens. Matter **23**, 094217 (2011).
[6] K. Miyake and S. Watanabe, J. Phys. Soc. Jpn. **83**, 061006 (2014).
[7] H. Q. Yuan, F. M. Grosche, M. Deppe, C. Geibel, G. Sparn, and F. Steglich, Science **302**, 2104 (2003).
[8] Z. Ren, L. V. Pourovskii, G. Giriat, G. Lapertot, A. Georges, and D. Jaccard, Phys. Rev. X **4**, 031055 (2014).
[9] H. Hegger, C. Petrovic, E. G. Moshopoulou, M. F. Hundley, J. L. Sarrao, Z. Fisk, and J. D. Thompson, Phys. Rev. Lett. **84**, 4986 (2000).
[10] G. F. Chen, K. Matsubayashi, S. Ban, K. Deguchi, and N. K. Sato, Phys. Rev. Lett. **97**, 017005 (2006).
[11] M. Yashima, S. Kawasaki, H. Mukuda, Y. Kitaoka, H. Shishido, R. Settai, and Y. Onuki, Phys. Rev. B **76**, 020509(R) (2007).
[12] G. Knebel, D. Aoki, J. P. Brison, and J. Flouquet, J. Phys. Soc. Jpn. **77**, 114704 (2008).
[13] T. Park, V. A. Sidorov, F. Ronning, J.-X. Zhu, Y. Tokiwa, H. Lee, E. D. Bauer, R. Movshovich, J. L. Sarrao, and J. D. Thompson, Nature (London) **456**, 366 (2008).
[14] H. Shishido, R. Settai, H. Harima, and Y. Onuki, J. Phys. Soc. Jpn. **74**, 1103 (2005).
[15] S. Watanabe and K. Miyake, J. Phys. Soc. Jpn. **79**, 033707 (2010).
[16] A.-S. Ruetschi and D. Jaccard, Rev. Sci. Instrum. **78**, 123901 (2007).
[17] B. Cornut and B. Coqblin, Phys. Rev. B **5**, 4541 (1972).
[18] A. D. Christianson, J. M. Lawrence, P. G. Pagliuso, N. O. Moreno, J. L. Sarrao, J. D. Thompson, P. S. Riseborough, S. Kern, E. A. Goremychkin, and A. H. Lacerda, Phys. Rev. B **66**, 193102 (2002).
[19] A. D. Christianson, A. H. Lacerda, M. F. Hundley, P. G. Pagliuso, and J. L. Sarrao, Phys. Rev. B **66**, 054410 (2002).
[20] Y. Matsumoto, K. Kuga, T. Tomita, Y. Karaki, and S. Nakatsuji, Phys. Rev. B **84**, 125126 (2011).
[21] The temperature windows for the fitting are $1.2\ \mathrm{K} < T < T_N$ at $p = 0$, $T_c < T < T_N$ between 1.03 and 1.78 GPa, $T_c < T < 6$ K between 1.94 and 3.80 GPa, and $1.2\ \mathrm{K} < T < 6$ K above 4.02 GPa.
[22] K. Miyake and O. Narikiyo, J. Phys. Soc. Jpn. **71**, 867 (2002).
[23] Note that, for the c-axis case, θ tends to ∞ since $T_{cr} \sim 0$. Hence h/θ is not physically meaningful.
[24] M. Yashima, N. Tagami, S. Taniguchi, T. Unemori, K. Uematsu, H. Mukuda, Y. Kitaoka, Y. Ōta, F. Honda, R. Settai, and Y. Ōnuki, Phys. Rev. Lett. **109**, 117001 (2012).
[25] P. G. Pagliuso, R. Movshovich, A. D. Bianchi, M. Nicklas, N. O. Moreno, J. D. Thompson, M. F. Hundley, J. L. Sarrao, and Z. Fisk, Physica B **312-313**, 129 (2002).
[26] T. C. Kobayashi, K. Fujiwara, K. Takeda, H. Harima, Y. Ikeda, T. Adachi, Y. Ohishi, C. Geibel, and F. Steglich, J. Phys. Soc. Jpn. **82**, 114701 (2013).